Extended Wide-Bandwidth Rogowski Current Sensor with PCB Coil and Electronic Characteristic Shaper

Li, He; Xin, Zhen; Li, Xue; Chen, Jianliang; Loh, Poh Chiang; Blaabjerg, Frede

Published in:
I E E E Transactions on Power Electronics

DOI (link to publication from Publisher):
10.1109/TPEL.2020.3001058

Publication date:
2021

Document Version
Accepted author manuscript, peer reviewed version

Extended Wide-Bandwidth Rogowski Current Sensor with PCB Coil and Electronic Characteristic Shaper

He Li, *Student Member*, *IEEE*, Zhen Xin, *Member*, *IEEE*, Xue Li, Jianliang Chen, *Member*, *IEEE*, Poh Chiang Loh, and Frede Blaabjerg, *Fellow*, *IEEE*

***Abstract*-Because of their fast switching speeds, current measurements for wide band-gap (WBG) devices have become increasingly challenging. Particularly, the designed current sensor must be nonintrusive and have a small size and a very wide bandwidth. One promising current sensor is the printed-circuit-board (PCB) Rogowski current sensor, whose bandwidth is wide only if parasitic parameters of its measuring coil are minimized prominently. This is presently achieved by reducing the number of turns of the coil, which undesirably will degrade its signal-to-noise ratio. Alternatively, an electronic characteristic shaper proposed in this letter can be used for neutralizing parasitic effects, while performing integration to restore the measured current. Theoretical analyses and experimental results have shown that the resulting Rogowski current sensor does indeed have a wider bandwidth, even without changing its measuring coil.**

***Index Terms*—PCB Rogowski coil, wide band-gap device, current measurement, power electronics**

I. Introduction

Compared to traditional silicon devices, power converters implemented with WBG devices, such as silicon carbide (SiC) metal-oxide-semiconductor field-effect transistors (MOSFETs), have a faster switching speed [1] and a higher power density [2]. Those features, in turn, demand current sensors for measuring currents through the WBG devices to be nonintrusive with both a wide high-frequency bandwidth and a small footprint. Precise short-circuit protection [3] and current monitoring [4] can then be implemented with such high-end current sensors. The development of such sensors is however non-trivial with most existing sensors, including coaxial shunt, current transformer, and Hall-effect sensor, being not directly applicable.

For instance, with the coaxial shunt, although its bandwidth can reach the unmatchable GHz range, its bulkiness is unquestionably not ideal for raising power density. Current transformer, with a bandwidth as high as tens of MHz, can next be considered, especially since it has widely been used for AC current sensing [5]. Its non-intrusiveness is however not ideal, because of its high-frequency parasitic inductance. The third option is the popular Hall-effect sensor, whose bandwidth is nonetheless always below 1 MHz due to possible saturation of its magnetic core. It is thus similarly not ideal for WBG devices.

Instead, a Rogowski current sensor, with a Rogowski coil and an integrator, has more recently been suggested as a promising sensor, since it satisfies all three requirements below:

1) It has a wide high-frequency bandwidth, since it does not use a magnetic core and hence does not experience magnetic saturation.

2) It is nonintrusive, since it detects only a small amount of magnetic fluxes for measurement, while using no magnetic core for flux concentration.

3) It is small in size, especially when implemented with tracks and vias on a printed-circuit-board (PCB).

Therefore, a PCB Rogowski current sensor can indeed be the optimal choice. This may also be the reason for [6] to use it for measuring switching current through a laminated bus bar. Various concerns however still exist with the Rogowski current sensor. One of them is its coil parasitic components, which like parasitic in all sensors, introduce limitations. One limitation is the lowering of bandwidth below a certain resonant frequency, which for a Rogowski coil, has commonly been solved by reducing its number of turns or size. For example, in [7], a single-turn coil has been proven to have a bandwidth as high as 1 GHz. It is however at the expense of a smaller, and hence less accurate, signal-to-noise ratio. High bandwidth and high signal-to-noise ratio are therefore not mutually achievable by only changing the coil structure.

Instead, greater tuning flexibilities may be achieved through modifying its processing electronics, which conventionally have been designed to only integrate the coil output. The coil output, in turn, is a scaled derivative of the measured current. Together, the coil and integrator can then restore a scaled copy of the current for measurement. Using a pure integrator only has however not resolved the tradeoff between bandwidth and signal-to-noise ratio through proper circuit design.

Therefore, this letter proposes a new electronic characteristic shaper, whose main purpose is to shape frequency responses of the overall Rogowski current sensor. The shaped frequency responses then offer a wider and higher bandwidth without

Manuscript received April 10, 2020; accepted May 31, 2020. This work was supported in part by the Youth Program of National Natural Science Foundation of China under Grants 51907048, in part by the Green Channel Program of Natural Science Foundation of Hebei Province under Grant E2019202345, and in part by the Youth Top Talent Program of Department of Education of Hebei Province under Grant BJ2019043. (*Corresponding author: Zhen Xin*)

He Li, Zhen Xin, Xue Li and Jianliang Chen are with the State Key Laboratory of Reliability and Intelligence of Electrical Equipment, Hebei University of Technology, Tianjin 300130, China (email: 201921401088@stu.hebut.edu.cn; xzh@hebut.edu.cn; lixue@ hebut.edu.cn; chenjl@hebut.edu.cn).

Poh Chiang Loh is with Department of Electronic Engineering, the Chinese University of Hong Kong, Hong Kong SAR, China (email: epcloh@ gmail.com).

Frede Blaabjerg is with Department of Energy Technology, Aalborg University, Aalborg, Denmark (email: fbl@et.aau.dk).

This article has been accepted for publication in a future issue of this journal, but has not been fully edited. Content may change prior to final publication. Citation information: DOI 10.1109/TPEL.2020.3001058, IEEE Transactions on Power Electronics

demanding for lesser coil turns. Effectiveness of the shaping has been verified experimentally with a Bode-100 frequency analyzer. Subsequently, experimental measurement of a 10-MHz current using the shaped current sensor has been performed to demonstrate its accuracy over a conventional unshaped Rogowski current sensor. It should however be clarified that the proposed shaper is not like [8] and others, where a Rogowski coil and another sensing technique have been combined to create a hybrid current sensor. Such hybrid sensor does have a wider bandwidth, but achieved by lowering its lower bound, rather than raising its upper bound like the proposed shaper.

II. Basic Measuring Principles

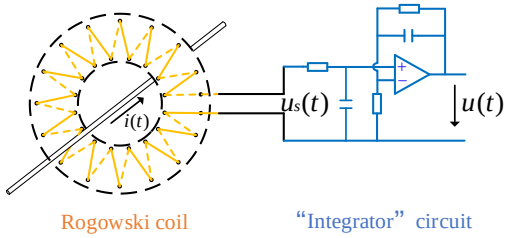

Fig. 1. A typical Rogowski current sensor with coil and integrator.

A typical Rogowski current sensor consists of a coil and an integrator, as depicted in Fig. 1. The coil can be routed on a PCB for detecting derivative of the primary measured current $i(t)$, according to:

$$u_s(t) = M\frac{di}{dt} \qquad (1)$$

where $u_s(t)$ is the output voltage and M is the mutual inductance of the coil. Magnitude response of the coil is thus a straight line rising at +20 dB/dec, while its phase response is a constant at 90°. These responses are however not achievable in practice, due to non-zero parasitic inductance and capacitance. An illustration of parasitic influences can be seen from Fig. 2(a),

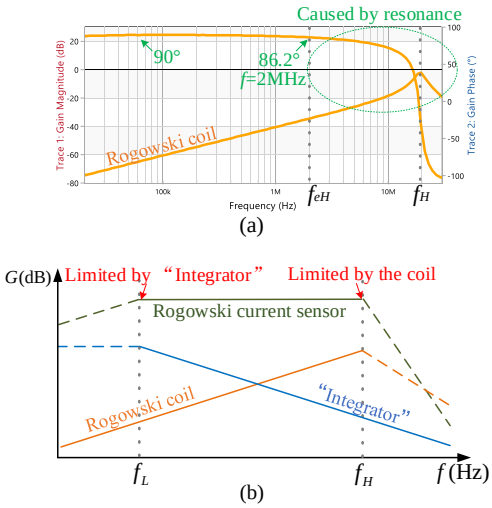

Fig. 2. Frequency responses of (a) Rogowski coil only and (b) Rogowski current sensor.

measured with a Bode-100 frequency analyzer. Unique features observed from the figure are the presence of a resonant peak at f_H = 19 MHz and the start of phase roll-off to 86.2° at f_{eH} = 2 MHz. An upper limit contributed by the coil therefore exists, and is usually regarded as f_H, even though the phase roll-off starts earlier at f_{eH}.

The coil output is then fed to an integrator, which in practice, usually has a low-pass characteristic and a cutoff frequency marked as f_L in Fig. 2(b). It is therefore only capable of restoring the measured current above f_L, but below f_H due to parasitic of the coil. The outcome is then a constant-gain region between f_L and f_H in Fig. 2(b) for the overall current sensor. The constant gain can next be used to determine the current measuring range as $I_{Min} \le i \le U_{Max}/(MK)$, where I_{Min} is a value satisfying specified signal-to-noise ratio, U_{Max} is the maximum voltage that the integrator can output (determined by power supply of op-amp), and K is the integral gain. Moreover, as observed from Fig. 2(b), the immediate challenge is to increase f_H, in order to measure current through the WBG device. Conventionally, the increase has been achieved by reducing the number of turns to lower parasitic inductance of the coil. However, lesser turns inevitably lowers signal-to-noise ratio of the sensor. Therefore, a new electronic characteristic shaper has been proposed to resolve the tradeoff, as detailed next.

III. Electronic Characteristic Shaper

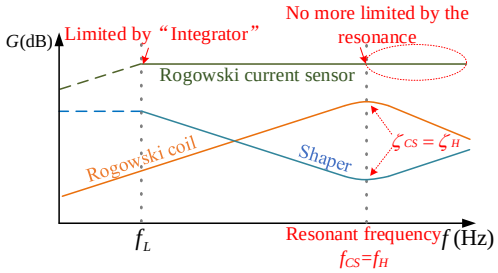

Fig. 3. Frequency responses of damped coil, characteristic shaper and shaped Rogowski current sensor with widened bandwidth.

A. Underlying Principles

Instead of performing integration only, the electronic circuit after the coil can provide characteristic shaping to widen the constant-gain (and 0°-phase) bandwidth beyond f_H in Fig. 2(b). It is therefore appropriate to name the circuit as a shaper with the same low-pass characteristic, as indicated in Fig. 3. However, at f_H, the response of the shaper arcs back to create a trough for cancelling resonant peak of the coil, if their damping ratios are also set equal. Beyond f_H, the shaper, behaving like a differentiator, continues to cancel the coil roll-off. The shaped frequency response of the current sensor in Fig. 3 therefore has a significantly lifted (ideally infinite) high-frequency bound, not achieved by reducing turns of the coil.

B. Coordinated Design of Characteristic Shaper

From earlier, the characteristic shaper must provide:

1) Integration below resonant frequency f_H.

2) Cancellation at f_H and beyond.

This article has been accepted for publication in a future issue of this journal, but has not been fully edited. Content may change prior to final publication. Citation information: DOI 10.1109/TPEL.2020.3001058, IEEE Transactions on Power Electronics

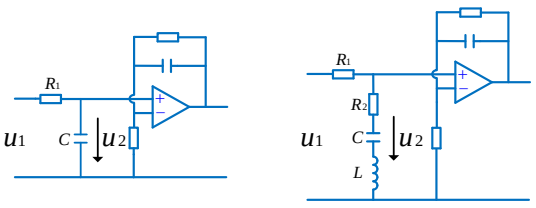

(a) (b)

Fig. 4. Schematics of (a) hybrid integrator and (b) characteristic shaper.

The first requirement can be ensured by adopting the conventional hybrid integrator shown in Fig. 4(a) [9], from which Fig. 4(b) can be derived to meet the second requirement simultaneously. Therefore, beginning with Fig. 4(a), the hybrid integrator can be sized independently as a front passive RC integrator connected to a rear active non-inverting integrator [10]. The non-inverting integrator is for low-frequency integration, while the RC integrator is for high-frequency integration. No interaction exists between them, since the non-inverting terminal of the rear op-amp does not draw any significant current from the front RC circuit.

Modifications should therefore only be introduced to the front passive circuit to provide the necessary high-frequency cancellation expected from the shaper. The exact modifications introduced to Fig. 4(b) are the addition of inductor L for series-resonating with integrating capacitor C, and resistor R_2 for tuning its damping ratio. Transfer function of the front passive circuit can thus be expressed as:

$$\frac{u_2}{u_1} = \frac{s^2LC + sCR_2 + 1}{s^2LC + sC(R_1 + R_2) + 1} \tag{2}$$

from which resonant frequency f_{CS} and damping radio ζ_{CS} of the shaper can be derived as:

$$f_{CS} = \frac{1}{2\pi} \cdot \sqrt{\frac{1}{LC}} \tag{3}$$

$$\zeta_{CS} = \frac{CR_2}{2\sqrt{LC}} \tag{4}$$

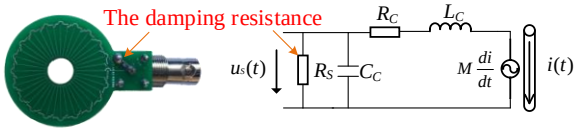

(a) (b)

Fig. 5. Illustration of (a) physical construction and (b) lumped-parameter model of Rogowski coil.

These expressions must match those of the 40-turn differential PCB coil, wound according to [11] to provide high noise immunity. Physical layout and model of the coil are shown in Fig. 5(a) and (b), respectively. The latter includes R_c, C_c and L_c for modeling parasitic of the coil, whose values can be computed using existing techniques, like in [12], or measured. Together, they give rise to a resonant peak, whose damping radio can be adjusted by an external resistor R_s, also included in the figure. Transfer function of the damped coil can then be expressed as:

$$\frac{u_S}{i} = -\frac{sMR_s}{s^2L_cC_cR_s + s(L_c + C_cR_cR_s + C_cR_s^2) + R_c + R_s} \tag{5}$$

from which resonant frequency f_H and damping radio ζ_H of the coil can be derived as:

$$f_H = \frac{1}{2\pi} \cdot \sqrt{\frac{R_c + R_s}{L_cC_cR_s}} \tag{6}$$

$$\zeta_H = \frac{C_cR_s^2 + C_cR_cR_s + L_c}{2\sqrt{L_cC_cR_cR_s + L_cC_cR_s^2}} \tag{7}$$

Cancellation can eventually be achieved by enforcing:

$$f_{cs} = f_H \quad \text{and} \quad \zeta_{cs} = \zeta_H \tag{8}$$

IV. Experimental Results

To prove the newly shaped frequency responses, an experimental setup with a Bode-100 analyzer has been assembled, as shown in Fig. 6(a). The setup includes a 10-Ω sampling resistor for converting the measured current into a voltage signal for feeding to CH1. The ratio of output of the shaper to the sampled signal (CH2/CH1) then gives frequency responses of the sensor. Subsequently, the setup in Fig. 6(b) has been used to display waveforms measured with the PCB Rogowski current sensor with and without shaping.

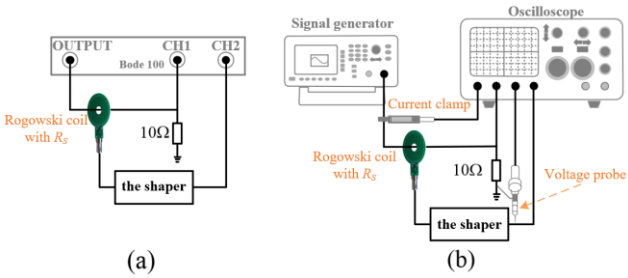

(a) (b)

Fig. 6. Experimental setups for measuring (a) frequency response with Bode-100 analyzer and (b) actual high-frequency waveform.

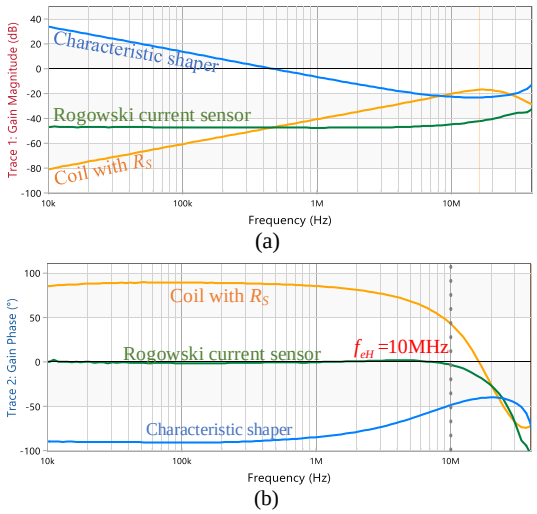

Fig. 7. Measured (a) magnitude and (b) phase responses of shaped Rogowski current sensor.

This article has been accepted for publication in a future issue of this journal, but has not been fully edited. Content may change prior to final publication. Citation information: DOI 10.1109/TPEL.2020.3001058, IEEE Transactions on Power Electronics

A. Measurements with Bode-100 *Analyzer*

The measured coil and its frequency responses are shown in Fig. 5(a) and Fig. 2(a), respectively. Its measured parasitic parameters are $R_C = 3.96\Omega$ and $L_C = 949.5\text{nH}$, which together with resonant frequency read from Fig. 2(a), give rise to a parasitic capacitance of $C_C = 70\text{pF}$. These parameters, upon substituted to (7), gives rise to a damping ratio ζ_H for each chosen damping resistance R_s. The final chosen damping parameters are $R_S = 120\ \Omega$ and $\zeta_H = 0.986$ to provide a fully damped coil characteristic for easier cancellation by the shaper. The shaper in Fig. 4(b) has, in turn, been found to have parameters $L = 2.2\ \mu\text{H}$, $C = 40\ \text{pF}$, $R_1 = 20.25\ \text{k}\Omega$ and $R_2 = 462\ \Omega$ to satisfy (8). However, R_2 has subsequently been changed to $543\ \Omega$, after fine-tuning measured frequency responses of the combined current sensor.

The resulting measured magnitude and phase responses of the shaped current sensor are shown in Fig. 7(a) and (b) respectively. Fig. 7(a) shows the cancellation of resonant peak of the coil, while Fig. 7(b) shows the retention of 0° phase until a much higher frequency. To better demonstrate the latter, Fig. 8 shows phase responses of the shaped current sensor and conventional current sensor without shaping and damping resistor R_s in Fig. 5. More specifically, Fig. 8 shows phase of the conventional sensor starting to deviate from 0° at around 2 MHz, which according to Fig. 2(a), is the same as observed with the PCB coil alone. This is expected, since as explained in

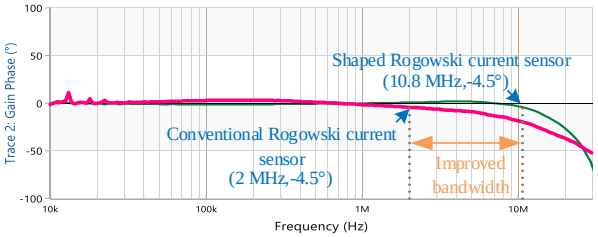

Fig. 8. Phase responses of conventional and shaped Rogowski current sensor.

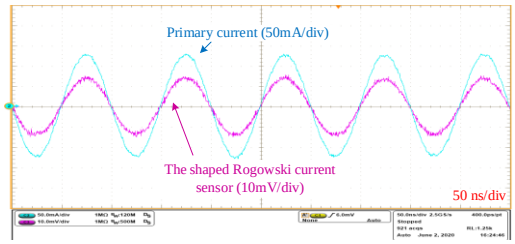

(a)

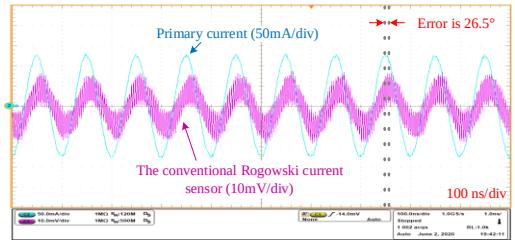

(b)

Fig. 9. Measured current and output waveforms of (a) shaped and (b) conventional Rogowski current sensors at 10 MHz.

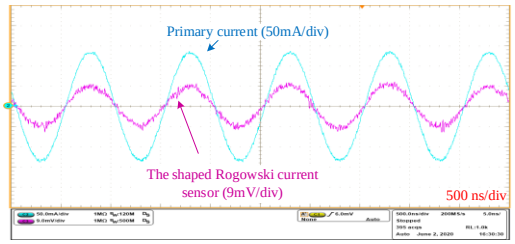

(a)

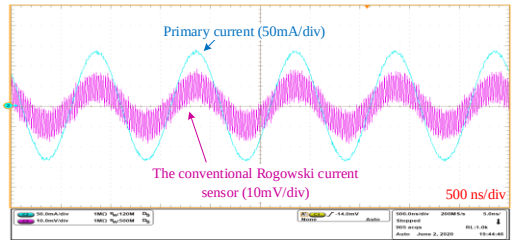

(b)

Fig. 10. Measured current and output waveforms of (a) shaped and (b) conventional Rogowski current sensors at 1 MHz.

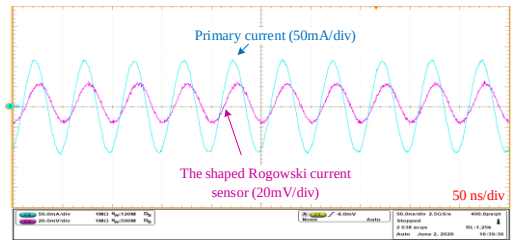

(a)

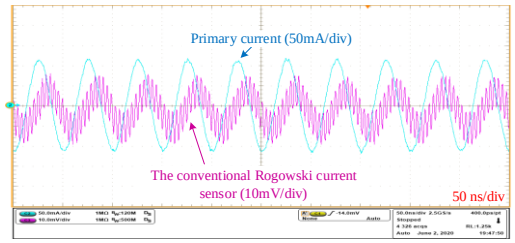

(b)

Fig. 11. Measured current and output waveforms of (a) shaped and (b) conventional Rogowski current sensors at 20 MHz.

Section II, integrator of the conventional sensor will not influence upper bound of its bandwidth. In contrast, phase of the shaped current sensor begins to deviate from 0° only from about 10 MHz onwards. Effectiveness of the shaper has therefore been demonstrated.

B. Measurement with 10-MHz Primary Current

To further strengthen verification of the proposed method, both conventional and shaped current sensors have been positioned, as in Fig. 6(b), to measure a 130-mA primary current at 10 MHz. Fig. 9(a) shows the primary current and output of the shaped current sensor, which apparently are in phase. In contrast, Fig. 9(b) shows the same primary current, but now with a 26.5°-phase-shifted output from the conventional current sensor. This phase shift is expected, since effective bandwidth of the conventional sensor is only up to 2

MHz, as compared to 10 MHz of the shaped current sensor with the same PCB coil.

Bandwidths of both sensors have also been verified by results included in Fig. 10 and Fig. 11. Fig. 10 is for 1 MHz within the bandwidths of both sensors. Their respective outputs therefore have no phase errors with reference to the measured primary current. In contrast, Fig. 11 shows both sensors producing phase errors, since their common tested frequency of 20 MHz is beyond their respective bandwidths. Meanwhile, outputs of the conventional sensor in Fig. 9(b) to Fig. 11(b) are noted to be more oscillatory at around 240 MHz, which in Fig. 9(a) to Fig. 11(a), has been damped by resistor R_2 of the shaper in Fig. 4(b). This resonance and other imperfections due to parasitic of the op-amp, connecting tracks and others have however only been resistively damped, rather than properly reshaped. They are also not captured by the Bode-100 analyzer, because of its 50-MHz upper limit. They have hence not been cancelled by adding more RLC branches to the non-inverting terminal of the shaper in Fig. 4(b).

V. Conclusion

This letter proposes a redesigned Rogowski current sensor with an electronic characteristic shaper. The shaper is for cancelling a properly damped resonance from the coil and shaping its high-frequency responses, in addition to providing integration for restoring the primary current. The resulting shaped current sensor then has a much wider bandwidth, which in experiments, has an upper bound that is five times higher that of the conventional current sensor. The shaped current sensor therefore does not have to tradeoff between wide bandwidth and high signal-to-noise ratio, while retaining its simplicity. It is thus a suitable current sensor for measuring current through a WBG device in a highly dense power converter.

References

[1] R. Mitova, R. Ghosh, U. Mhaskar, D. Klikic, M.-X.Wang, and A. Dentella, "Investigations of 600-V GaN HEMT and GaN diode for power converter applications," *IEEE Trans. Power Electron*., vol.29, no.5, pp.2441–2452, May 2014.

[2] Y.-F. Wu, J. Gritters, L. Shen, R. P. Smith, and B. Swenson, "kV-class GaN-on-Si HEMTs enabling 99% efficiency converter at 800 V and 100 kHz," *IEEE Trans. Power Electron*., vol. 29, no. 6, pp. 2634–2637, Jun. 2014.

[3] J. Wang, Z. Shen, R. Burgos, and D. Boroyevich, "Design of a high bandwidth Rogowski current sensor for gate-drive short circuit protection of 1.7 kV SiC MOSFET power modules," in *Proc. IEEE Work. Wide Bandgap Power Devices. Appl*., pp. 104–107, 2015.

[4] C. Hewson and J. Aberdeen, "An improved Rogowski coil configuration for a high speed, compact current sensor with high immunity to voltage transients," in *Proc. IEEE Appl. Power Electron. Conf. Expo*., pp. 571–578, 2018.

[5] C. Xiao, L. Zhao, T. Asada, W.G. Odendaal and J.D. van Wyk, "An overview of integratable current sensor technologies," in *Proc. IEEE. 38th IAS Annu. Meeting Conf. Rec. Ind. Appl. Conf.*, pp. 1251–1258, Oct. 2003.

[6] Y. Kuwabara, K. Wada, J. Guichon, J. Schanen, and J. Roudet, "Implementation and Performance of a Current Sensor for a Laminated Bus Bar," in *IEEE Trans. Ind. Appl*, vol. 54, no. 3, pp. 2579-2587, May-June 2018.

[7] C. Luo et al., "Collocated and simultaneous measurements of RF current and voltage on a trace in a noncontact manner," *IEEE Trans. Microw. Theory Techn*., vol. 67, no. 6, pp. 2406–2415, Jun. 2019

[8] T. Funk, J. Groeger and B. Wicht, "An Integrated and Galvanically Isolated DC-to-15.3 MHz Hybrid Current Sensor," *IEEE Appl. Power Electron. Conf. Expo*., pp.1010-1013, Mar. 2019

[9] J. A. J. Pettinga and J. Siersema, "A polyphase 500 kA current measuring system with Rogowski coils," *IEE Pro-Electril Power Appl.*, vol. 130, no. 5, pp. 360-363, 2013.

[10] W. F. Ray and C. R. Hewson, "High performance Rogowski current transducers," in *Proc. IEEE Ind. Appl. Conf*., pp. 3083– 3090, Oct. 2000.

[11] J. N. Fritz, C. Neeb, and R. W. De Doncker, "A PCB integrated differential Rogowski Coil for non-intrusive current measurement featuring high bandwidth and dv/dt immunity," in *Proc. Power and Energy Student Summit*, S05. 2, 2015.

[12] V. Dubickas and H. Edin, "High-frequency model of the Rogowski coil with a small number of turns," *IEEE Trans. Instrum. Meas.*, vol. 56, no. 6, pp. 2284–2288, Dec. 2007.